PASJ: Publ. Astron. Soc. Japan **46**, L65–L70 (1994)

ASCA Observation of Three Bright Early-Type Galaxies: NGC 4472, NGC 4406, and NGC 4636

Hisamitsu AWAKI,[1] Richard MUSHOTZKY,[2] Takeshi TSURU,[1] Andrew C. FABIAN,[3] Yasushi FUKAZAWA,[4] Michael LOEWENSTEIN,[2] Kazuo MAKISHIMA,[4] Hironori MATSUMOTO,[1] Kyoko MATSUSHITA,[4] Tatehiro MIHARA,[5] Takaya OHASHI,[6] George R. RICKER,[7] Peter J. SERLEMITSOS,[2] Yoshiyuki TSUSAKA,[8] and Takashi YAMAZAKI[8]

[1] *Department of Physics, Faculty of Science, Kyoto University, Sakyo-ku, Kyoto 606-01*
[2] *Laboratory for High Energy Astrophysics, NASA/GSFC, Greenbelt, MD 20771, USA*
[3] *Institute of Astronomy, University of Cambridge, Madingley Road, Cambridge, CB3 0HA, UK*
[4] *Department of Physics, School of Science, University of Tokyo, Bunkyo-ku, Tokyo 113*
[5] *The Institute of Physical and Chemical Research, 2-1 Hirosawa, Wako, Saitama 350-01*
[6] *Department of Physics, Faculty of Science, Tokyo Metropolitan University, Hachioji, Tokyo 192-03*
[7] *Center for Space Research, Massachusetts Institute of Technology, Cambridge, MA 02139, USA*
[8] *Department of Physics, Faculty of Science, Nagoya University, Chikusa-ku, Nagoya 464-01*

(Received 1994 February 8; accepted 1994 March 26)

Abstract

We report ASCA 0.3–10 keV X-ray observations of three early type galaxies, NGC 4472, NGC 4406, and NGC 4636. The extended emission in these galaxies is well described by thin thermal emission from hot gas. The gas temperature is 0.92 ± 0.02 keV for NGC 4472, 0.79 ± 0.01 keV for NGC 4406, and 0.73 ± 0.02 keV for NGC 4636. The metal abundance for NGC 4472, NGC 4406, and NGC 4636 are, under the assumption of solar ratios, 0.63 ± 0.15, 0.45 ± 0.10, and 0.38 ± 0.07, respectively. Detailed analysis has allowed determination of the abundances of oxygen, silicon, sulfur, and iron. The observed abundances are consistent with the solar ratios. For NGC 4472 and NGC 4406 we also determined the mean temperature of the gas producing the Si lines from the ratio of the Si H to He-like lines and find it to be consistent with the continuum temperature. The X-ray temperature is in good agreement with the observed optical velocity dispersion, stellar density profile, and gas density profile. Our data indicates that the supernova rate should be less than one fifth of the nominal rate in early type galaxies. We derive the mass of these systems within fixed angular scales and find that $M/L > 40$, confirming that elliptical galaxies are dark matter dominated at large radii.

Key words: Early type galaxies — Galaxies: abundances — Galaxies: individual (NGC 4472, NGC 4406, NGC 4636) — X-rays: galaxies

1. Introduction

Observations with the Einstein observatory IPC revealed the existence of extended X-ray emission around optically luminous early type galaxies (Forman et al. 1985) whose origin was thought to be emission from hot gas. The gas temperature was estimated to be ~ 1 keV, and the typical gas mass is 10^9–$10^{10} M_\odot$, corresponding to a few percent of the stellar mass.

The origin of such a large amount of gas and its heating mechanism are not well understood. It is thought that the hot gas is due, primarily, to mass loss from evolved stars heated by shocks due to relative stellar motions, by gravitational compression, and by type Ia supernova shocks. Determination of the gas temperature and the abundances of the gas can strongly constrain the origin of the gas and its evolutionary history (Renzini et al. 1993, David et al. 1991). Previous measurements of the temperature and abundance of ellipticals (Serlemitsos et al. 1993, Forman et al. 1993) suffered from rather low signal to noise or poor energy resolution.

ASCA (Tanaka et al. 1994) carries imaging spectrometers with high energy resolution and has a large effective area in the wide energy band from 0.3 to 10 keV. In this energy band, there are numerous emission lines from all the low Z abundant elements with the strongest lines being due to oxygen, silicon, sulfur, and iron. Measurement of the intensity of these lines allows determination of the metal abundance in the hot gas. We report preliminary analysis of three of the brightest elliptical galaxies, NGC 4472, NGC 4406, and NGC 4636.

Table 1. Characteristics of the target galaxies.

Target	Position	$\log(L_B/L_\odot)^*$	$M_{gas}/M_\odot^\dagger$	σ (km s^{-1})§
NGC 4472	(12h29m46s, 7°57′57″)	11.13	2.1×10^{10}	310 ± 7
NGC 4406	(12h26m12s, 12°56′47″)	10.81	2.5×10^{10}	253 ± 7
NGC 4636	(12h42m50s, 2°41′17″)	10.42	0.8×10^{10}	227 ± 12

* at D=20 Mpc for NGC 4472 and NGC 4406, and D=16 Mpc for NGC 4636.
† Forman et al. 1985
§ Davies et al. 1983

Table 2. Summary of the X-ray observations.

Target	Date	Instrument (mode)*	Exposure (ks)	Diameter	Net counts (cts s^{-1})	BGD (cts s^{-1} arcmin^{-2})
NGC 4472	1993 July 04	SIS(F/B,4/4)	19	5′	0.22	8×10^{-4}
NGC 4406	1993 July 03	SIS(F/F,4/2)	20	6′	0.25	21×10^{-4}
NGC 4636	1993 June 22	SIS(F/B,4/4)	18	8′	0.23	5×10^{-4}

* bit rate high/bit rate medium, F: faint mode, B: bright mode, 4: 4CCD mode, 2: 2CCD mode

2. ASCA Observations

NGC 4472, NGC 4406, and NGC 4636 were observed with the ASCA satellite during the PV phase, and both the SIS data (Burke et al. 1992) and the GIS data (Ohashi et al. 1991) were obtained from the galaxies. The characteristics for the galaxies and a log of the observations are summarized in table 1 and table 2, respectively. Because its higher energy resolution and higher efficiency below 1 keV result in having a much increased sensitivity to line emission from 1 keV plasmas, in this analysis only the SIS data are used. We chose the data taken with 4CCD mode in faint mode, and then we followed the "nominal" data analysis procedures. In table 2 we give the background subtracted counts within the circles centered at the X-ray centroid position and with the specified extraction radii. In figure 1 we show the spectra after the background subtraction.

It is well known that the Virgo cluster has an extending X-ray emission, and the surface brightness at the positions of NGC 4406 and NGC 4472 in the 0.2 keV to 4.0 keV band is roughly 1×10^{-14} erg s^{-1} cm^{-2} arcmin^{-2} and 1×10^{-15} erg s^{-1} cm^{-2} arcmin^{-2}, respectively (Fabricant, Gorenstein 1983). The latter value is of the same order as the SIS background. For NGC 4472, we used as background a region 15′ from the center of the galaxy, where the surface brightness of the galaxy is about one tenth of the background level. For NGC 4406, a field between NGC 4406 and NGC 4374 was selected as the background region, to avoid the contamination from the X-ray structure around NGC 4406. Since NGC 4636 is very far from M87, it is free from the gas emission of the Virgo cluster and thus background subtraction is straightforward.

3. Spectral Analysis

Since the SIS signal is very weak at $E > 5$ keV, we restricted our analysis to the 0.4 keV to 5 keV band. The spectra from the individual detectors are fitted with separate responses but, with the exception of normalization, the spectral parameters were constrained to be the same. The spectra were fitted with both χ^2 and maximum likelihood methods with the XSPEC spectral fitting package. Generally, both methods gave consistent results, and we give only the results from the χ^2 method.

Thin thermal plasma models (Raymond, Smith 1977) modified by interstellar absorption with solar abundance ratios were fit to each galaxy. The fitting results are shown in table 3. For this model the reduced χ^2 is less than 1.5 for all three galaxies. The gas temperature for each galaxy lies in a narrow range from 0.7 keV to 0.9 keV, and is slightly smaller than those measured with the Einstein IPC (Trinchieri et al. 1986 hereafter TFC). The temperature for NGC 4636 agrees, within the errors, with the Ginga results but our best fit temperature for NGC 4472 is significantly less than that determined by Ginga (Awaki et al. 1991). This difference is accounted for by the hard component seen in the ASCA spectra (Matsushita et al. 1994) (see below).

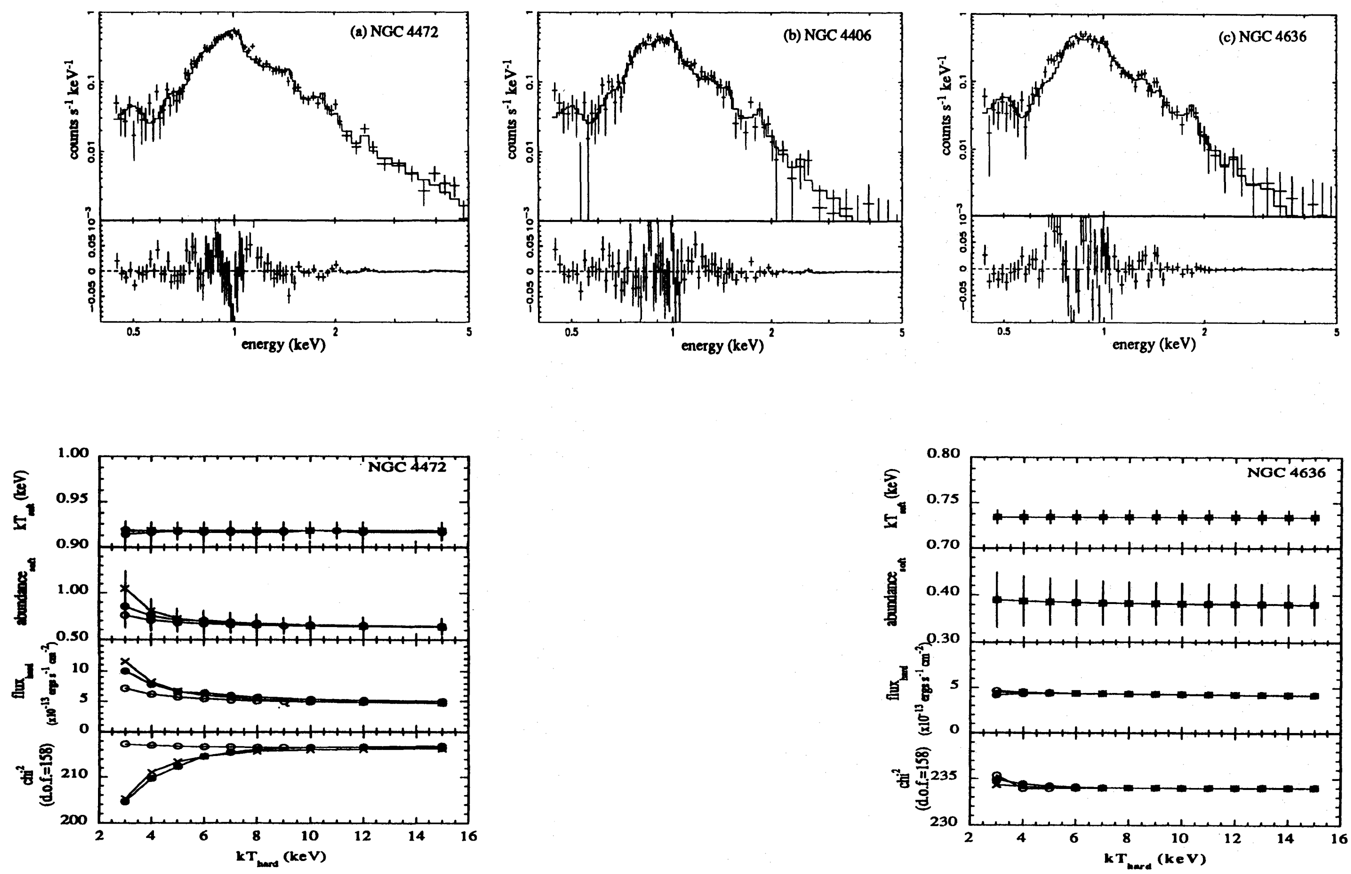

Fig. 1. The upper figures show the pulse height spectra with the SIS from NGC 4472 (a), NGC 4406 (b), and NGC 4636 (c). The histogram shows the best fitting (R-S plasma + high temperature bremsstrahlung) model. The lower figures show the dependence of the low kT component on the temperature of the hard emission for NGC 4472 (a), and NGC 4636 (c). Open circles, filled circles, and crosses stand for the metal abundances of zero, unity, and the same as the soft component.

We note that our results, especially the abundance, can be sensitive to the background spectrum. If a position near the target galaxies is used as the background position, the results will be different, because the X-ray emission at radii less than 10′ contains the emission from the target galaxies. We have found from both the SIS and GIS data that there exists a hard spectral component which grows stronger relative to the low temperature component at larger radii. This component is the most likely cause of the higher Ginga temperatures. We have selected as background a region far enough away from the centers of these galaxies where this hard component is very weak and thus believe that our results are not strongly sensitive to the background used.

A detailed analysis of the excess emission in the high energy band with the GIS sensor is presented in Matsushita et al. (1994). They find that the excess emission can be described by a thermal model with temperature $kT > 2$ keV and that the X-ray luminosity lies on the relationship between blue band luminosity ($L_{\rm B}$) and X-ray luminosity ($L_{\rm X}$) seen in spiral galaxies. Since it seems that the excess emission comes from the discrete sources in the galaxies, we fixed the spectral shape, and determined the intensity of the hard component via spectral fitting. The best fitted parameters are listed in table 3. The intensity of the excess emission is consistent with the GIS fit. The possibility that the excess emission comes from hot gas can not be ruled out. The temperature of the hard emission can affect the abundances derived in the soft component. We show the dependence of the low kT component parameters on the hard emission in figure 1. For NGC 4406, since only upper limit of the hard emission is derived in any temperature, the dependence is not obtained. We note that the abundance for NGC 4472 is greater than unity, if the temperature of the hard emission is taken to be 3 keV.

The abundance of the abundant elements in the two component model (R-S plasma +high temperature bremsstrahlung) was allowed to be a free parameter (table 3). The fitted abundances are all similar and con-

Table 3. The best fit parameters and 90% confidence region of an interest.

	NGC 4472	NGC 4406	NGC 4636
Flux (0.5–4.5 keV) (erg s^{-1} cm^{-2})	6.1×10^{-12}	4.8×10^{-12}	6.6×10^{-12}
N_H (10^{22} cm^{-2})	0.15 (0.14–0.17)	0.10 (0.08–0.13)	0.08 (0.07–0.10)
kT (keV)	0.92 (0.90–0.93)	0.79 (0.78–0.80)	0.73 (0.72–0.74)
Abundance*	0.51 (0.44–0.59)	0.45 (0.38–0.56)	0.35 (0.30–0.40)
χ^2 (Raymond)	228.1 (160)	183.7 (160)	229.3 (160)
N_H (10^{22} cm^{-2})	0.12 (0.10–0.14)	0.10 (0.06–0.11)	0.07 (0.05–0.09)
kT (keV)	0.92 (0.90–0.93)	0.79 (0.78–0.80)	0.73 (0.72–0.75)
Abundance*	0.63 (0.52–0.79)	0.45 (0.37–0.58)	0.38 (0.32–0.45)
Flux of high energy component .... (10^{-12} erg s^{-1} cm^{-2}in 0.5–4.5 keV)	0.5 (0.24–0.8)	0.0 (0.0–0.2)	0.4 (0.1–0.7)
χ^2	216.6 (159)	183.7 (159)	225.7 (159)
N_H (10^{22} cm^{-2})	0.18 (0.15–0.20)	0.11 (0.06–0.16)	0.12 (0.09–0.16)
kT (keV)	0.94 (0.92–0.95)	0.77 (0.70–0.80)	0.60 (0.56–0.64)
Abundance O†	0.20 (0.00–0.50)	0.68 (0.09–1.58)	0.23 (0.10–0.42)
Si†	0.22 (0.14–0.31)	0.44 (0.25–0.82)	0.32 (0.24–0.40)
S†	0.40 (0.23–0.58)	0.42 (0.00–1.14)	0.40 (0.00–0.76)
Fe†	0.52 (0.45–0.61)	0.47 (0.30–0.71)	0.20 (0.18–0.27)
Flux of high energy component .... (10^{-12} erg s^{-1} cm^{-2}in 0.5–4.5 keV)	0.2 (0.0–0.5)	0.05 (0.0–0.3)	0.70 (0.35–1.05)
χ^2	160.5 (151)	174.9 (151)	210.74 (151)

∗ Thin thermal model with the same ratio to the solar abundance by Raymond and Smith.
† Thin thermal model with independent variables for abundances.

sistent with the total abundance. In particular we note that the O/Fe ratio is consistent with solar values. We also were able to measure the temperature sensitive H to He like line ratio of Si in both NGC 4472 and NGC 4406. These ratios of 0.66 (1.1, 0.36) in NGC 4472 and 0.3 (0.7, 0.04) in NGC 4406 at 90% confidence are consistent with the observed continuum temperatures and indicate that much of the gas is in equilibrium and close to isothermal.

We note that there is a significant line-like residual around 0.7 keV remaining in the best fit of two temperature model for NGC 4636 and NGC 4472. It is not caused by the background events nor by atmospheric fluorescence. Fitting it with a narrow gaussian profile, the flux in this line is 3×10^{-4} photons s^{-1} cm^{-2} in NGC 4636 and 1–2 $\times$ 10^{-4} photons s^{-1} cm^{-2} in NGC 4472. This feature may be attributed to O and Fe blends from a thermal plasma with $kT < 0.35$ keV. We believe that this line is not an artifact of the detector response function or data analysis techniques since it does not appear in other sources of similar intensity and is seen in both detectors for the two galaxies with low absorption.

The derived values of abundance, temperature, and column density for NGC 4472 are quantitatively in good agreement with the BBXRT values (Serlemitsos et al. 1993), and qualitatively confirms the recently published ROSAT analysis of Forman et al. (1993). The analysis of the radial profile of the ASCA abundance and kT values is in progress and will be presented at a later date.

4. Discussion

In the most popular scenario, the amount of the hot gas in elliptical galaxies is produced by mass loss from evolved stars (cf. Loewenstein, Mathews 1987), because the stellar mass loss rate is much larger than the gas ejection by supernovae. The gas can be heated by relative stellar motions, by adiabatic compression in an inflow through the gravitational potential, and by supernova explosions, especially type Ia supernovae (hereafter SN Ia). Since the iron is mainly produced by the SN Ia, the iron abundance $N_{\rm Fe}$ in the hot gas should be determined by the combination of the mass loss and the SN Ia rate, i.e.,

$$N_{\rm Fe} = \frac{\frac{dM}{dt} \times N_{\rm Fe,mass\ loss} + r_{\rm SN\ Ia} \times M_{\rm Fe,SN\ Ia}}{\frac{dM}{dt} + r_{\rm SN\ Ia} \times M_{\rm SN\ Ia}} \quad (1)$$

We use as standards the specific SN Ia rate of $r_{\rm SN\,Ia}$ = 0.22 SN/100 yr/$10^{10}L_{\odot}$ (Tammann et al. 1982), $M_{\rm SN\,Ia} = 1.4M_{\odot}$, the energy in the explosion ($E_{\rm SN\,Ia}$) of 6×10^{50} erg and 0.6 $M_{\odot}$ of Fe ejected from one SN Ia

(Nomoto et al. 1984). We have assumed that the total rate of mass ejected in the galaxies from mass loss is $dM/dt \sim 1.5\times10^{-11} L_{\rm B} M_{\odot}/{\rm yr}$ (Knapp et al. 1992) which is consistent with the presently observed total gas mass of these systems integrated over 10^{10} yr.

The observed upper limit on the Fe abundance (0.71) constrains the SN Ia rate (Loewenstein, Matthews 1991). The stellar contribution to the total metallicity is estimated from the absorption structure in optical band, and it is about one solar abundance (e.g., Worthey et al. 1992). However there is an ambiguity of the stellar metallicity, because it can not be estimated in optical band, directly. Therefore, for these galaxies, we set it to zero to derive an absolute upper limit to $r_{\rm SN\ Ia}$, which is to < 0.2 of the Tammann rate. We note that the metallicity estimated from optical data is consistent with ASCA spectra, if $r_{\rm SN\,Ia} = 0$. Since the total luminosity due to supernova heating is

$$L_{\rm SN\ Ia} = r_{\rm SN\ Ia} \times E_{\rm SN\ Ia} \times L_{\rm B} \sim 4.1 \times 10^{41} \left(\frac{r_{\rm SN\ Ia}}{0.22}\right) \left(\frac{E_{\rm SN\ Ia}}{6\times10^{50}\ {\rm erg}}\right) \left(\frac{L_{\rm B}}{10^{11} L_{\odot}}\right) {\rm erg\ s^{-1}}, \tag{2}$$

the predicted X-ray luminosity is $< 8.2\times10^{40}$ erg s^{-1} per 10^{11} $L_{\rm B}$ and thus is less than 1/4 of the observed specific X-ray luminosity of any of these galaxies (which range from 1.5–3.0 $\times$ 10^{41} erg s^{-1}).

We thus find that SN Ia's are insignificant contributors to the total energy budget in elliptical galaxies indicating that the primary heating mechanism is relative stellar motions and adiabatic compression in an inflow through the gravitational field.

The gas ejected from the evolved stars has a kinetic energy associated with the velocity dispersion of the stars. The ejected gas would encounter other gas, and be thermalized. In detail, if the gas and stars are in hydrostatic equilibrium in the same potential

$$T_{\rm X} \frac{d{\rm log}\rho}{d{\rm log}r} = T_{\rm stars} \frac{d{\rm log}N_{\rm stars}}{d{\rm log}r} \tag{3}$$

This equation is equivalent to the use of the "isothermal beta model." We define $\beta_{\rm image} = 3\beta_{\rm fit}/q$, where $q = d\log N_{\rm stars}/d\log r$ and $\beta_{\rm fit}$ is the fitted β for the X-ray image. The stellar density slope at $\sim 3R_{\rm e}$ (the effective radius of the integrated X-ray spectra) is 2.5, 2.4, and 3.0 and the gas density slope is 1.5, 1.35, 1.35 for NGC 4472, NGC 4406, and NGC 4636 respectively (TFC). The predicted gas temperatures are $T_{\rm X} \sim 1.0$, 0.71, and 0.72 keV which is in excellent agreement with the observations. In alternative language we find that there is excellent agreement between $\beta_{\rm spec} = T_{\rm stars}/T_{\rm X} = (0.60, 0.56, 0.45)$ and $\beta_{\rm image}$ (0.65, 0.51, 0.43) for NGC 4472, NGC 4406, and NGC 4636, respectively. Given that the optical velocity dispersions are central values and the X-ray temperature is heavily weighted towards larger radii this strongly suggests that the optical velocity dispersion is not decreasing at larger radii.

Table 4. X-ray determined total mass.

Galaxy	R (kpc)*	$M(\times 10^{12} M_{\odot})$	$M/L_{\rm B}$
NGC 4472	80	4.2 ± 0.4	45
NGC 4406	88	3.2 ± 0.4	72
NGC 4636	44	1.6 ± 0.2	52

* Forman et al. 1985

The observed central column density in each galaxy is larger than the galactic values and is similar to the value inferred from the IPC analysis by TFC. The "extra" absorption is similar to that seen by ASCA in the Centaurus cluster (Fukazawa et al. 1994) and in other cooling flow clusters by the Einstein SSS (White et al 1991). This has been attributed to the accumulation of cold material by a cooling flow. In the case of NGC 4472, the rather large amount of material implied [$M_{\rm cold} \sim 3\times10^{10} M_{\odot}(R/25\ {\rm kpc})^2 \times (N_{\rm H}/15\ \times 10^{20}\ {\rm H\ cm^{-2}})$] is marginally consistent with the observed cooling rate $\sim$ 1–2 $M_{\odot}$/yr (Thomas et al. 1986) for 15×10^9 yr and represents a major sink of gas in these systems.

Using our accurate temperature measurements we can estimate the gravitational mass in these systems (table 4). The M/L values are $\sim$ 3–4 larger than the central M/L values (Lauer 1985) and indicate the increasing dominance of dark matter at larger radii.

The observed "solar" abundance ratio of low Z elements to Fe is not expected in most evolutionary models of elliptical galaxies (Renzini et al. 1993). In particular the O/Fe ratio is inconsistent with models dominated by type I SN. The abundance ratio implies a galactic ratio of type I SN and type II SN, and indicates that the observed X-ray emitting gas would have not been recently produced in these objects, because there are essentially no massive stars now existing in giant ellipticals. The evolution of X-ray emitting gas have to be recalculated.

We thanks all the member of the ASCA team. We also thank Professor K. Koyama for discussion and reading of the manuscript and Dr. S. Ichikawa for his kind help. This research has made use of the NASA/IPAC Extragalactic Database (NED) which is operated by the Jet Propulsion Laboratory, California Institute of Technology, under contract with the National Aeronautics and Space Administration. This work was partly supported by the Scientific Research Fund of the Ministry of Education, Science, and Culture under Grant No. 05452020 (T.T.) and No. 05242104 (T.T.).

References

Awaki H., Koyama K., Kunieda H., Takano S., Tawara Y., Ohashi T. 1991, ApJ 366, 88

Burke B.E., Mountain R.W., Harrison D.C., Bautz M.W., Doty J.P., Ricker G.R., Daniels P.J. 1991, IEEE Trans. ED-38, 1069

David L.P., Forman W., Jones C. 1991, ApJ 380, 39

Davies R.L., Efstathiou G., Fall S.M., Illingworth G., Schechter P.L. 1983, ApJ 266, 41

Fabricant D., Gorenstein P. 1983, ApJ 267, 535

Forman W., Jones C., David L., Franx M., Makishima K., Ohashi T., Tucker W. 1993, ApJL 418, L55

Forman W., Jones C., Tucker W. 1985, ApJ 293, 102

Fukazawa Y. et al. 1994, PASJ 46, L55

Knapp G.R., Gunn J.E., Wynn-Williams C.G. 1992, ApJ 399, 76

Lauer T.R. 1985, ApJ 292, 104

Loewenstein M., Mathews W.G. 1987, ApJ 319, 614

Loewenstein M., Mathews W.G. 1991, ApJ 373, 445

Matsushita K., Makishima K., Awaki H., Canizares C.R., Fabian A.C., Fukazawa Y., Loewenstein M., Matsumoto H. et al. 1994, ApJL submitted

Nomoto K., Thielemann F.-K., Yokoi, K. 1984, ApJ 286, 644

Ohashi T., Makishima K., Ishida M., Tsuru T., Tashiro M., Mihara T., Kohmura Y., Inoue H. 1991, Proc SPIE 1549, 9

Raymond J.C., Smith B.W. 1977, ApJS 35, 419

Renzini A., Ciotti L., D'Ercole A., Pellegrini S. 1993, ApJ 419, 52

Serlemitsos P.J., Loewenstein M., Mushotzky R.F., Marshall F.E., Petre R. 1993, ApJ 413, 518

Tammann G.A. 1982, in Supernovae: A Survey of Current Research, ed. M.J. Rees, R.J. Stoneham (Dordrecht, Reidel) p371

Tanaka Y., Inoue H., Holt S.S. 1994, PASJ 46, L37

Thomas P, Fabian A.C., Arnaud K.A., Forman W., Jones C. 1986, MNRAS 222, 655

Trinchieri G., Fabbiano G., Canizares C.R. 1986, ApJ 310, 637 (TFC)

van den Bergh S., McClure R.D., Evans, R. 1987, ApJ 323, 44

Warthey G., Faber S.M., Gonzalez J.J. 1992, ApJ 398, 69

White D., Fabian A., Johnstone R., Mushotzky R., Arnaud K.A. 1991 MNRAS 252, 72